

# Relative stability of $\text{Si}_n$ and $\text{Si}_n\text{Sc}^-$ clusters in the range $n = 14$ – $18$

M.B. Torres<sup>1,a</sup> and L.C. Balbás<sup>2</sup>

<sup>1</sup> Departamento de Matemáticas y Computación, Universidad de Burgos, Spain

<sup>2</sup> Departamento de Física Teórica, Atómica y Óptica, Universidad de Valladolid, Spain

Received 24 August 2006 / Received in final form 6 September 2006

Published online 24 May 2007 – © EDP Sciences, Società Italiana di Fisica, Springer-Verlag 2007

**Abstract.** We present a first-principles pseudopotential optimization of the lower energy equilibrium structure of  $\text{Si}_n\text{Sc}^-$  anions for  $n = 14$ – $18$ . We find that  $\text{Si}_{16}\text{Sc}^-$  is more stable than its neighbors clusters, in agreement with recent experimental mass spectra. We also optimize the geometry of pure  $\text{Si}_n$  neutral clusters in the range  $n = 14$ – $18$ , and compare our results with those from previous first-principles calculations.

**PACS.** 36.40.Cg Electronic and magnetic properties of clusters – 36.40.Qv Stability and fragmentation of clusters

## 1 Introduction

The evolution with size of the electronic and structural properties of pure and doped silicon nanoclusters is being studied intensively because the electronic devices are approaching to the nanoscale [1]. Structural information, inferred from a variety of experimental measurements [2–5] and computational studies [1, 6–13], states that the shape of low-lying isomers of  $\text{Si}_n$  are mostly prolate for  $n < 27$  and became near spherical for  $n > 27$ . In the range  $n = 10$ – $18$  nearly all clusters contain the tricapped-trigonal-prism (TTP) motif ( $\text{Si}_9$  subunit) [1, 5]. A recent calculation [8] obtained new global minimum of  $\text{Si}_{16}$  and low-lying isomers of  $\text{Si}_{17}$ ,  $\text{Si}_{18}$  and  $\text{Si}_{22}$  built on a different generic motif based on the  $\text{Si}_6$  tetragonal bipyramid and the  $\text{Si}_6$  sixfold puckered ring structural subunits. Another recent result, using a refined structural optimization method [10], regain the TTP motif as the ground state of  $\text{Si}_{16}$  instead of the six/six structural motif. On the experimental side, photoelectron spectroscopy (PES) spectra are used, when is possible, to elucidate the geometry of these clusters [5]. Moreover, the morphology of the ground state for  $\text{Si}_n$  and  $\text{Si}_n^+$  clusters in the range  $n = 14$ – $20$  can be different than for  $\text{Si}_n^-$  [5].

Concerning the growth behavior of transition metal-doped silicon clusters, recent first-principles calculations [14] have found that open basketlike structures are the most favorable for  $n = 8$ – $12$ , while for  $n = 13$ – $16$  the metal atom becomes completely surrounded by Si atoms. For  $n = 16$  results the optimal cage for the metal-encapsulated silicon clusters. In a recent mass spectrometry experiment [15], Nakajima and coworkers have

shown the size-selective formation of  $\text{Si}_{16}\text{Sc}^-$ ,  $\text{Si}_{16}\text{Ti}$ , and  $\text{Si}_{16}\text{V}^+$  clusters.

In this work we present first-principles computational studies of the relative stability of  $\text{Si}_n\text{Sc}^-$  anions for  $n = 14$ – $18$ . We find that  $\text{Si}_{16}\text{Sc}^-$  is more stable than its neighbors clusters, in agreement with the experiment [15]. We have performed also an optimization of the geometry of pure  $\text{Si}_n$  neutral clusters in the range  $n = 14$ – $16$ . In Section 2, we outline briefly the computational method, in Section 3, we present and discuss the results. In Section 4, conclusions are given.

## 2 Computational methods

We use the first-principles code SIESTA [16] to solve fully self-consistently the standard Kohn-Sham equations [17] of DFT within the GGA as parametrized by Perdew, Burke and Ernzerhof [18]. We use norm conserving scalar relativistic pseudopotentials [19] in their fully nonlocal form [20], generated from the atomic valence configuration  $3s^23p^2$  for Si (with core radii 1.9 a.u. for  $s$  and  $p$  orbitals), and the semi-core valence configuration  $4s^23p^63d^1$  for Sc (with core radii, in a.u., 2.57, 1.08, and 1.37 for  $s$ ,  $p$ , and  $d$  orbitals, respectively). Flexible linear combinations of numerical (pseudo) atomic orbitals are used as the basis set, allowing for multiple- $\zeta$  and polarization orbitals. In order to limit the range of the basis pseudoatomic orbitals (PAO), they are slightly excited by a common energy shift (0.068 eV in this work), and truncated at the resulting radial node. In the present calculations we used a double- $\zeta$  basis ( $s, p$  for Si, and  $s, p, d$  for Sc), adding a single polarization orbital ( $d$  for Si and  $p$  for Sc). The maximum

<sup>a</sup> e-mail: mbtorres@yahoo.es

cutoff radii are 7.47 a.u. (for  $p$  of Si) and 8.85 a.u. (for  $s$  of Sc). The basis set of Sc was used and tested in references [21,22].

The basis functions and the electron density are projected onto a uniform real space grid in order to calculate the Hartree and exchange-correlation potentials and matrix elements. The grid fineness is controlled by the energy cutoff of the plane waves that can be represented in it without aliasing (120 Ry in this work).

To obtain the equilibrium geometries, an unconstrained conjugate-gradient structural relaxation using the DFT forces [23] was performed for several initial structures (typically more than twenty) until the force on each atom was smaller than  $0.010 \text{ eV/\AA}$ . For  $\text{Si}_n\text{Sc}^-$  anions we start with several geometries for doped  $\text{Si}_n\text{TM}$  isomers (TM = transition metal) obtained in previous works [14,24,25], and we also use our optimized low-lying geometries of neutral  $\text{Si}_n$  adding a  $\text{Sc}^-$  at different sites, as well as other configurations that we invented. For pure  $\text{Si}_n$  we optimize the low-lying isomeric geometries which we previously obtained using a genetic algorithms code [26], as well as those suggested by previous calculations [1,8,10,27], and many other variants of these which we have imagined.

### 3 Results and discussion

#### 3.1 $\text{ScSi}_n^-$ anions ( $n = 14-18$ )

In Figure 1 is represented the geometry of the lower energy isomer of  $\text{Si}_n\text{Sc}^-$  clusters for  $n = 14-18$ . In all these cases the Sc impurity is surrounded by Si atoms. The common structural motif, except for  $n = 15-16$ , is a distorted hexagonal prism (DHP) of Si atoms, which can be also viewed as two intertwined trigonal prisms, surrounding the Sc impurity, and subsequent Si atoms and dimers are added around the lateral prism faces. This DHP structure resembles the isomers  $C_s$  (ground state) and  $C_{2h}$  reported recently for  $\text{Si}_{12}\text{Ni}$  [28].

In our lower energy isomer for  $n = 14$  the DHP structure is decorated with a  $\text{Si}_2$  dimer. That structure is similar to the first isomer of  $\text{ZrSi}_{14}$  found in reference [29] (which is the second isomer of  $\text{ZrSi}_{14}$  found in Ref. [25]). The cubic structure for neutral  $\text{FeSi}_{14}$  obtained in references [30,31], is a stable isomer of  $\text{Si}_{14}\text{Sc}^-$  with 1.42 eV excess energy. Our ground state for  $\text{Si}_{15}\text{Sc}^-$  is similar to the second isomer of  $\text{Si}_{15}\text{Ti}$  in reference [14] and to the third isomer of  $\text{Si}_{15}\text{Cr}$  in reference [24]. For  $\text{Si}_{16}\text{Sc}^-$  we obtain the Frank-Kasper (FK) polyhedral structure obtained previously for  $\text{Si}_{16}\text{Ti}$  and  $\text{Si}_{16}\text{Hf}$  [14,30]. This is a more compact, near spherical, geometry. For  $\text{Si}_{17}\text{Sc}^-$ , a dimer and a trimer binds the lateral faces of the DHP motif, and for  $\text{Si}_{18}\text{Sc}^-$  three silicon dimers decorate alternating lateral faces of the DHP structure. These geometries can not be related to the neutral pure clusters  $\text{Si}_{17}$  and  $\text{Si}_{18}$  given in reference [8,10].

In the inset of Figure 1 we plot the second difference of the cluster energy,

$$\Delta_2 E_n = E_{n+1} + E_{n-1} - 2E_n,$$

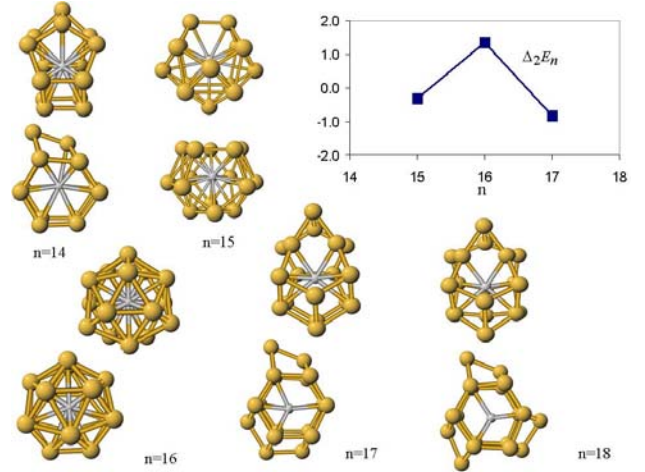


**Fig. 1.** Two views of the geometry of the lower energy isomer of  $\text{Si}_n\text{Sc}^-$  anions for  $n = 14-18$ . The small sphere represents the Sc atom. In the inset is plotted the second derivative of the total cluster energy, showing a positive peak at  $n = 16$  as a signature of the special stability detected in experiments [12].

**Table 1.** Binding energy per atom ( $E_b$ , in eV), addition energy of a  $\text{Sc}^-$  anion to  $\text{Si}_n$  ( $E_{\text{Sc}^-}^{\text{ad}}$ , in eV), addition energy of a Si atom to a  $\text{Si}_{n-1}\text{Sc}^-$  anion ( $E_{\text{Si}}^{\text{ad}}$ , in eV), the Homo-Lumo Gap ( $\Delta_n^{\text{gap}}$ , in eV), and the average distance Sc-Si (in  $\text{\AA}$ ), for the lower energy state of  $\text{Si}_n\text{Sc}^-$  anions.

$n$	$E_b$	$E_{\text{Sc}^-}^{\text{ad}}$	$E_{\text{Si}}^{\text{ad}}$	$\Delta_n^{\text{gap}}$	$d_{\text{av}}^{\text{Sc-Si}}$
14	4.19	8.32		0.65	2.90-2.83
15	4.21	8.65	4.63	0.92	2.88
16	4.25	10.03	4.95	2.12	2.87
17	4.22	9.29	3.60	0.78	3.12-2.97
18	4.23	9.60	4.42	0.81	3.23-3.08

where  $E_n$  is the total energy of the  $\text{Si}_n\text{Sc}^-$  cluster. This second difference is proportional to  $\log(I_n/I_{n+1})$ , where  $I_n$  is the intensity of the  $\text{Si}_n\text{Sc}^-$  signal in the experimental mass spectra [32]. We see in Figure 1 that  $\Delta_2 E_n$  is negative for  $n = 15$  and  $n = 17$ , and is positive for  $n = 16$ , corresponding to the peak detected at  $n = 16$  in the experiments [15].

In Table 1 is given the binding (atomization) energy per atom of  $\text{Si}_n\text{Sc}^-$ ,

$$E_b(n) = [E(\text{Sc}^-) + nE(\text{Si}) - E_n(\text{Si}_n\text{Sc}^-)]/(n+1),$$

the addition energy of a  $\text{Sc}^-$  anion to a  $\text{Si}_n$  cluster,

$$E_{\text{Sc}^-}^{\text{ad}}(n) = E(\text{Si}_n) + E(\text{Sc}^-) - E_n(\text{Si}_n\text{Sc}^-),$$

the addition energy of a Si atom to a  $\text{Si}_{n-1}\text{Sc}^-$  anion,

$$E_{\text{Si}}^{\text{ad}}(n) = E(\text{Si}_{n-1}\text{Sc}^-) + E(\text{Si}) - E_n(\text{Si}_n\text{Sc}^-),$$

and the energy difference between the LUMO and HOMO orbital eigenvalues,  $\Delta_n^{\text{gap}}$ , of the  $\text{Si}_n\text{Sc}^-$  cluster. The second difference energy,  $\Delta_2 E_n$ , is equivalent to  $E_{\text{Si}}^{\text{ad}}(n) - E_{\text{Si}}^{\text{ad}}(n+1)$ . As for this second difference, we see in Table 1 a peak at  $n = 16$  in  $E_b(n)$ , in  $E_X^{\text{ad}}(n)$  ( $X = \text{Sc}^-, \text{Si}$ ),

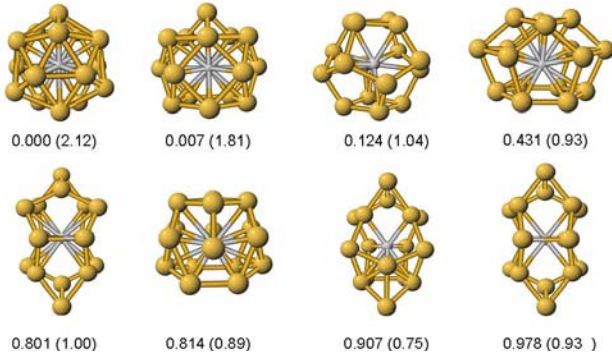


**Fig. 2.** Geometry of a few low energy isomers of  $\text{Si}_{16}\text{Sc}^-$ . The energy excess with respect to the lower energy isomer, and the Homo-Lumo gap (in parenthesis) are also given (in eV). Note the different specular structure of the host silicon cluster for the first and last isomers in the second row, which are related to the ground state structure of  $\text{Si}_{16}$  reported in references [1,26], respectively.

and in  $\Delta_n^{gap}$ . The average bond distance Sc-Si is also given in Table 1. Two distances are given, corresponding to consider in the average all atoms (first number) or only the first neighbors (second number). We see that  $\text{Si}_{16}\text{Sc}^-$  is more compact and with smaller distance Sc-Si than the other clusters.

The magnetic moment of the lower energy isomer of  $\text{Si}_n\text{Sc}^-$  in our calculations ( $n = 14-16$ ) is null. More details for other isomers will be given in a forthcoming publication [26]. The calculated vertical (adiabatic) electron detachment energy of  $\text{Si}_{16}\text{Sc}^-$  is 3.62 (3.29) eV, to be compared with the experimental value 4.25 (3.41) eV [15].

Several low energy isomers of  $\text{Si}_{16}\text{Sc}^-$  are represented in Figure 2. The excess energy with respect to the ground state and the Homo-Lumo gap are also given in Figure 2. The geometries of isomers 1, 3, and 5, are related to those of pure  $\text{Si}_{16}$  isomers or doped  $\text{Si}_{16}\text{TM}$  obtained in previous works [1,8,10,27,24,30,29], but the others are reported here for the first time.

### 3.2 Neutral $\text{Si}_n$ clusters ( $n = 14-18$ )

The geometries of the few lowest energy isomers of neutral  $\text{Si}_n$  clusters are represented in Figure 3. The binding energy per atom ( $E_b(n)$ ), the addition energy of a Si atom to a  $\text{Si}_n$  cluster ( $E^{ad}$ ), the second difference of the total energy ( $\Delta_2 E_n$ ), and the Homo-Lumo gap ( $\Delta_n^{gap}$ ), are given in Table 2 for the lower energy isomer.

The geometry for the lower energy isomer of  $\text{Si}_n$  in Figure 3, except for  $\text{Si}_{16}$ , is similar to the one reported by Ho and coworkers [1], and is based on the TTP motif. The first and second isomers of  $\text{Si}_{14}$  incorporate to the TTP a group of four Si atoms, and differs in the site where the fifth Si atom is added. The first isomer of  $\text{Si}_{15}$  is a TTP unit plus a ring of six atoms, similarly to the first isomer reported in references [1,7]. The second and third isomers of  $\text{Si}_{15}$  are the union of two TTP sharing a triangular face but

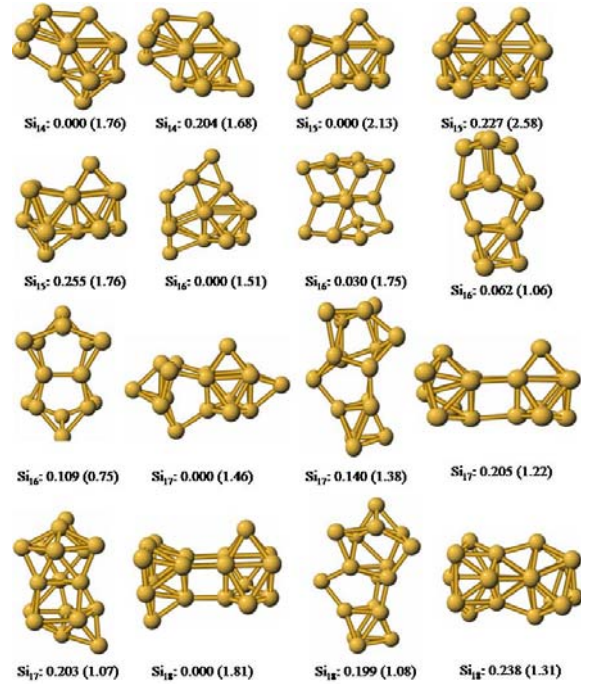


**Fig. 3.** Geometry of the few lowest energy isomers of  $\text{Si}_n$  clusters for  $n = 14-18$ . For each isomer is given (in eV) the excess energy with respect to the ground state and, in parenthesis, the Homo-Lumo gap.

**Table 2.** Binding energy per atom ( $E_b$ , in eV), addition energy of a Si atom to  $\text{Si}_n$  (in eV) the second derivative of the total energy ( $\Delta_2 E_n$ , in eV), and the Homo-Lumo Gap ( $\Delta_n^{gap}$ , in eV) for the lower energy state of silicon clusters. The  $E_b$  for the second isomer is given in parenthesis.

$n$	$E_b$	$E^{ad}$	$\Delta_2 E_n$	$\Delta_n^{gap}$
14	3.89 (3.87)			1.76
15	3.91 (3.90)	4.30	0.72	2.13
16	3.89 (3.89)	3.58	-0.76	1.51
17	3.92 (3.91)	4.34	0.22	1.46
18	3.93 (3.92)	4.12		1.81

with different orientations. To our knowledge, these two-TTP structures of  $\text{Si}_{15}$  are reported here for the first time, although they have some resemblance to the third and fourth isomers, respectively, reported by Zhu and coworkers [7]. Other new isomers of  $\text{Si}_{15}$  obtained within Siesta-LDA calculations are reported in reference [13]. Our first isomer of  $\text{Si}_{16}$  contains a TTP unit plus seven atoms, and is similar to the first isomer reported by Goedecker and coworkers [10]. Our second isomer of  $\text{Si}_{16}$  has a symmetric and compact structure which is similar to the second isomer in reference [10]. The third isomer of  $\text{Si}_{16}$  coincides with the first isomer obtained by Yoo and coworkers [8], and the fourth isomer coincides with the first isomer reported in references [1,7]. Our first isomer of  $\text{Si}_{17}$  coincides with the first isomer in references [1,10], while the second isomer of  $\text{Si}_{17}$  coincides with the first isomer in reference [8], and does not contain any TTP unit. The third

and fourth isomers of  $\text{Si}_{17}$  coincide with the isomers  $\text{Si}_{17a}$  and  $\text{Si}_{17b}$  reported in reference [10], which contain two separated TTP units and any TTP unit, respectively. The first, second, and third isomers of  $\text{Si}_{18}$  are similar to the first isomer of references [1, 8, 10], respectively.

Comparing the structures in Figures 1 and 2 with those in Figure 3 we see that there is not obvious relation between the  $\text{Si}_n\text{Sc}^-$  and  $\text{Si}_n$  or  $\text{Si}_{n+1}$  geometries, at least for the lower energy structures. On the other hand, comparing the values quoted in Tables 1 and 2 we remark the following facts. (i) The addition energy of a Si atom to a  $\text{Si}_n$  cluster is about a half the addition energy of a  $\text{Sc}^-$  anion, and in both cases is larger for  $n = 16$  than for the neighbor clusters. (ii) The second energy difference,  $\Delta_2 E_n$ , shows a positive peak for  $\text{Si}_{16}\text{Sc}^-$  (see Fig. 1), in agreement with the special stability detected in the experiment [15]. However, we obtain a negative peak for  $\text{Si}_{16}$ , contrary to the result in reference [12], but in agreement with the result of Li and coworkers [33]. This points to  $\text{Si}_{15}$  or  $\text{Si}_{17}$  as candidates to be *magic* clusters. In this respect, notice that experiments [34] have detected  $\text{Si}_{14}^+$  and  $\text{Si}_{18}^-$  as possible *magic* clusters. The binding energy of  $\text{Si}_n$  clusters with  $n = 14-18$  fits quite well the phenomenological expression [4, 35]  $E_b(n) = E_b(\infty) - cn^{-1/3}$ , where  $E_b(\infty)$  is the binding energy of bulk solid (experiment: 4.63 eV/atom; DFT-Siesta-PBE-DZbasis [16]: 4.84 eV/atom). From our values in Table 2 and  $E_b(\infty) = 4.84$  eV, we obtain the coefficient  $c = 2.34$  eV, to be compared with the value  $c = 2.23$  eV resulting from a fit to experimental data for  $\text{Si}_n$  clusters in the range  $n = 25-70$  [4, 35].

## 4 Conclusions

We have studied the lower energy equilibrium structures of  $\text{Si}_n$  and  $\text{Si}_n\text{Sc}^-$  clusters, in the range  $n = 14-18$ , by means of first-principles DFT optimization of several initial geometries resulting from a genetic algorithm calculation [26], from modifications of previously reported geometries, and from our own imagination. We find that  $\text{Si}_{16}\text{Sc}^-$  is more stable than its neighbors clusters, in agreement with experimental mass spectra [15]. The calculated vertical and adiabatic electron detachment energies of  $\text{Si}_{16}\text{Sc}^-$  agree also with the experiments [15]. The structure of the lower energy isomer of  $\text{Si}_n\text{Sc}^-$  anions, except for  $n = 15-16$ , is based on a distorted hexagonal prism surrounding the Sc impurity, with a belt of  $\text{Si}_2$  and  $\text{Si}_3$  units. The lower energy isomer of  $\text{Si}_{15}\text{Sc}^-$  has similar geometry than second isomer of  $\text{Si}_{15}\text{Ti}$  in reference [14] and third isomer of  $\text{Si}_{15}\text{Cr}$  of reference [24]. For  $\text{Si}_{16}\text{Sc}^-$  the structure is more compact and consist of the Frank-Kasper polyhedron reported previously for other doped  $\text{Si}_{16}\text{M}$  clusters [14, 29, 30].

For pure  $\text{Si}_n$  clusters with  $n = 14-18$  we obtain a few lowest energy structures which are similar to those reported before [1, 7, 8, 10], but having different isomeric

order. We also obtain some low energy isomers which have not been reported before. Interestingly, the addition energy of a Si atom to a  $\text{Si}_n$  or a  $\text{Si}_n\text{Sc}^-$  cluster is smaller (near one half) than the addition energy of a  $\text{Sc}^-$  anion to a  $\text{Si}_n$  cluster.

We wish to acknowledge the support of the Spanish Ministry of Science (grant MAT2005-03415) and of FEDER of the European Community.

## References

1. K.-M. Ho et al., *Nature* **392**, 582 (1998)
2. E.C. Honea et al., *Nature* **366**, 42 (1993)
3. C.C. Arnold, D.M. Neumark, *J. Chem. Phys.* **99**, 3353 (1993)
4. M.F. Jarrold, E.C. Honea, *J. Phys. Chem.* **95**, 9181 (1991)
5. J. Müller et al., *Phys. Rev. Lett.* **85**, 1666 (2000)
6. N. Binggeli et al., *Phys. Rev. Lett.* **68**, 2956 (1992)
7. X.L. Zhu et al., *J. Chem. Phys.* **120**, 8985 (2004)
8. S. Yoo, X.C. Zeng, *Angew. Chem. Int. Ed.* **44**, 1491 (2005)
9. S. Yoo et al., *J. Am. Chem. Soc.* **126**, 13845 (2004)
10. S. Goedecker et al., *Phys. Rev. Lett.* **95**, 055501 (2005)
11. J. Bai et al., *J. Phys. Chem. A* **110**, 908 (2006)
12. M.A. Belkhir et al., *Physica E* **31**, 86 (2006)
13. S. Mahtout, M.A. Belkhir, *Acta Phys. Pol. A* **109**, 685 (2006)
14. H. Kawamura et al., *Phys. Rev. B* **71**, 075423 (2005)
15. K. Koyasu et al., *J. Am. Chem. Soc.* **127**, 4998 (2005)
16. J.M. Soler et al., *J. Phys.: Condens. Matter* **14**, 2745 (2002)
17. W. Kohn, L.J. Sham, *Phys. Rev.* **145**, 561 (1965)
18. J.P. Perdew et al., *Phys. Rev. Lett.* **77**, 3865 (1996)
19. N. Troullier, J.L. Martíns, *Phys. Rev. B* **43**, 1993 (1991)
20. L. Kleinman, D.M. Bylander, *Phys. Rev. Lett.* **438**, 1425 (1982)
21. E.M. Fernández et al., *Int. J. Quantum Chem.* **99**, 39 (2004)
22. M.B. Torres et al., *Phys. Rev. B* **71**, 155412 (2005)
23. L.C. Balbás et al., *Phys. Rev. B* **64**, 165110 (2001)
24. H. Kawamura et al., *Phys. Rev. B* **70**, 245433 (2004)
25. J. Wang, J.-G. Han, *J. Chem. Phys.* **123**, 064306 (2005)
26. M.B. Torres et al. (submitted); I. Martín-Bragado, Doctoral Dissertation, Universidad de Valladolid, 1994
27. The Cambridge Cluster Database, <http://www-wales.ch.cam.ac.uk/CCD.html>
28. E.N. Koukares et al., *Phys. Rev. B* **73**, 235417 (2006)
29. J. Lu, S. Nagase, *Phys. Rev. Lett.* **90**, 115506 (2003)
30. V. Kumar, Y. Kawazoe, *Phys. Rev. Lett.* **87**, 055503 (2001)
31. L. Ma et al., *Phys. Rev. B* **73**, 125439 (2006)
32. C.E. Klots, *J. Chem. Phys.* **92**, 5864 (1988)
33. B.-X. Li et al., *Phys. Lett. A* **316**, 252 (2003)
34. D.E. Bergeron, A.W. Castleman Jr, *J. Chem. Phys.* **117**, 3219 (2002)
35. T. Bachelis, R. Schafer, *Chem. Phys. Lett.* **324**, 365 (2000)